Charged particle Q values for reactions on C, Cr, Fe, Co, and Ni†

P. L. Jolivette, J. D. Goss, G. L. Marolt, A. A. Rollefson, and C. P. Browne
Department of Physics, University of Notre Dame, Notre Dame, Indiana 46556
(Received 3 July 1974)

Q values were measured for 27 reactions on targets of ^{12}C, ^{54}Cr, ^{54,56}Fe, ^{59}Co, and ^{58,60,62,64}Ni with resulting uncertainties of 0.7 to 3.2 keV. Care was taken to define sources of error. A χ^2 test on an interconnected set of 19 measurements indicates internal consistency and a comparison of eight (d,p) Q values with (n,γ) numbers shows excellent agreement. A mass evaluation was performed on a truncated region centered on Co. The results indicate that the 1971 values for the masses of ^{55}Cr and ^{55}Co are in error. The uncertainties of the masses of ^{53}Fe and ^{61}Co are greatly reduced. The question of the ^{57}Fe mass raised in The 1971 Atomic Mass Evaluation is not entirely resolved and consequently the absolute values of some masses in this region are still uncertain to about 5 keV although the Q values are improved.

[NUCLEAR REACTIONS ^{54,56}Fe, ^{59}Co, ^{58,60,62,64}Ni(p,α); ^{12}C, ^{54}Cr, ^{54,56}Fe, ^{59}Co, ^{58,60,62}Ni(d,p); ^{54,56}Fe, ^{59}Co, ^{60,62}Ni(d,t); ^{59}Co, ^{60,62}Ni(d,α); ^{54}Fe$(^3$He$,d)$; ^{54}Fe$(^3$He$,\alpha)$; ^{54}Fe, ^{59}Co(α,p) measured Q values. ^{12}C(d,d), (p,p) measured E_x. Mass adjustment.]

I. INTRODUCTION

The 1971 Atomic Mass Evaluation of Wapstra and Gove[1] (WG) resulted in masses and Q values for nuclei near stability with satisfactory precision for most purposes. However, since WG was published the masses of a number of light nuclei (^{15}O, ^{31}S, and ^{55}Co, for example[2]) have been found to be in error. It would not be surprising if other errors are present in such a large mass of data and indeed the data determining some primary nuclei, e.g. ^{49}Cr and ^{55}Cr, appear inconsistent. This particular investigation was started when we discovered that the ^{58}Ni$(p,\alpha)^{55}$Co Q value did not agree with the published value.[2] Furthermore, several areas of investigation such as the determination of the weak interaction vector coupling constant and isospin multiplet mass relations, have required even more precise masses through the p and s-d shells. An extension of Coulomb displacement energy studies into the f-p shell where the mass uncertainties are generally larger is feasible and could profit from better measurements throughout the shell, as will mass equations based on Coulomb energy or other considerations.

In the studies of cobalt isotopes being made at Notre Dame, accurate Q values are very useful. They do not strongly influence the accuracy of excited state energies because of the particular methods used, but are necessary to identify contaminants and in making comparisons with other reactions, particularly resonance reactions. Thus we decided to measure sufficient Q values to determine the mass differences for such reactions, especially as WG indicate that there is a possible systematic error in the region. A mass doublet measurement of ^{57}Fe is in disagreement with other values but cannot, apparently, be excluded on internal grounds. We hoped that further measurements might indicate if this doublet is correct.

In WG the most accurate reaction measurements in the upper f-p shell, ±2 keV or less, are $\Delta A = 0$, e.g., $\beta^{\pm}$ decay, e capture, and (p,n) or $\Delta A = 1$, e.g. (n,γ) and (p,γ). In contrast, for the Q values of greatest interest to us, $\Delta A = 2$ or 3, such as (d,α) and (p,α), no measurement in this region has an uncertainty of <5 keV while 10 keV or greater is the rule. Thus these Q values are determined through chains of more precise measurements resulting in uncertainties much larger than we can obtain directly. The additional precise cross links thus determined should increase confidence in the accuracy of the entire data set.

The relative newness of the 100 cm spectrograph[3] was a final consideration. We hoped that by making a series of conceptually simple experiments with various projectiles and outgoing particles and checking for both internal and external consistency we would find any residual inaccuracies. For this reason we took data on an interconnected cross linked set of nuclei which was subjected to statistical tests and on a number of (d,p) reactions which are compared with the very precise (n,γ) numbers which are available. In fact, we discovered that a correction, described below, to the measured magnetic field is required.

II. PROCEDURE

Beams were produced by the Notre Dame FN tandem Van de Graaff accelerator and reaction products analyzed with the 100 cm broad range spectrograph. The beam energy spread was limited to <0.05% by the analyzing magnet slits. Angular spread was <0.3° in the beam and <0.5° for the reaction products. Targets of enriched isotopes were prepared by vacuum evaporation on to 20 μg/cm^2 carbon backings and were 10–30 μg/cm^2 thick. All runs were taken at $\theta_{lab} = 90°$, with the targets in reflection geometry. Nuclear track plates were used as detectors.

Each run consists of three energy measurements: (1) the energy of the group elastically scattered from a heavy target for which $dE_{out}/dE_{in} \simeq 1$, $dE_{out}/d\theta$ is small, and E_{out} is sensitive to the beam energy; (2) the energy of the group elastically scattered from a light target for which $dE_{out}/dE_{in} < 1$, $dE_{out}/d\theta$ is large, and E_{out} determines the scattering angle; and (3) the energy of the reaction products leading to the ground and perhaps one to three of the lowest lying excited states of the final nucleus if they are precisely known (<1 keV). The heavy target was the target for the Q value and the light target ^{12}C. [For $^{12}C(d,p)^{13}C$ one of the other Q-value targets was used as the heavy target.] The uncertainties in the measured positions typically corresponded to $\Delta E_{in} < \pm 1$ keV and $\Delta\theta_{lab} < \pm 0.1°$. The elastic group from the heavy target was recorded simultaneously with the reaction particles unless the run was so long as to make the tracks uncountably dense. The elastic group from carbon was recorded in a separate run on a 10 μg/cm^2 carbon foil.

The intention was to take four runs for each Q value during at least two different running periods. This would reduce random uncertainties to $\simeq$1 keV and insure independence of the measurements. For certain reactions with small cross sections or low beam intensity fewer runs were taken.

III. ERROR ANALYSIS

The usefulness of the Q values measured lies in their precision and accuracy. Consequently, we have tried to make a complete and careful estimate of the uncertainties. The uncertainties are of three types: (1) Random errors that can be reduced by averaging over different final states of the residual nucleus in a single measurement. (An example is the error in counting each peak and determining its position.) (2) Errors that are common to all peaks in a given run but which can be averaged between runs, such as random errors in setting the magnetic field. (3) The systematic errors that are common to all runs, such as the uncertainty in the energy of ^{210}Po(α) used to calibrate the spectrograph. The uncertainties taken into account are listed in the first column of Table I and the type of error is given in the second column.

For each level of the final nucleus the measurements were reduced to ground state Q values and individual contributions to the random and systematic errors (see below and Table I) combined in quadrature. We realize, of course, that the individual systematic contributions may not be normally distributed. The best Q value was determined in two stages. First the Q values and errors for all levels seen in a single run were averaged. Then all runs were averaged. At each step the average was performed using a one parameter least squares fit:

$$\langle Q\rangle = \left(\sum_i Q_i/\sigma_{Ri}{}^2\right)\Big/\left(\sum_i 1/\sigma_{Ri}{}^2\right) \tag{1a}$$

$$\langle \sigma_R\rangle = \left(\sum_i 1/\sigma_{Ri}{}^2\right)^{-1/2} \tag{1b}$$

$$\langle \sigma_S\rangle = \left(\sum_i \sigma_{Si}/\sigma_{Ri}{}^2\right)\Big/\left(\sum_i 1/\sigma_{Ri}{}^2\right) \tag{1c}$$

$$\langle \sigma\rangle = (\langle \sigma_R\rangle^2 + \langle \sigma_S\rangle^2)^{1/2}, \tag{1d}$$

where Q_i are the Q values, σ_{Ri} is the random error in the measurement for this average, and σ_{Si} is the systematic error in the measurement. The random errors are reduced by repeated measurements and a weighted average of the systematic errors is taken.

The error algorithms are outlined below and Table I shows values for eight representative single runs.

A. Calibration and magnetic field

The spectrograph is calibrated using ^{210}Po(α) and ^{212}Po(α) sources. The magnetic rigidities used are 0.331 772 ± 0.000 003 Tm and 0.427 045 ± 0.000 002 Tm, respectively,[4] and all constants used are from Taylor, Parker, and Langenberg.[5] The sources were on 0.5 mm Ag wire to give an object that is the same height as the beam spot. The procedure is to place a series of particle groups along the focal surface by making small changes in the magnetic field which is determined with an NMR probe. The position (D) of the one-third height of the high energy side of the peak is measured and the relation between D and the radius of curvature (ρ) of the particle is then determined. The exit face of the magnet is cut in two circles and the rails holding the nuclear track plates were machined to a focal surface determined from the points of minimum

TABLE I. Typical uncertainties for single runs.

Uncertainty	Type [a]	Contribution to the uncertainty (keV)							
		$^{12}C(p,p')^{12}C$ (4.44 MeV)	$^{12}C(d,p)^{13}C$	$^{54}Fe(d,p)^{55}Fe$	$^{58}Ni(p,\alpha)^{55}Co$	$^{56}Fe(d,t)^{55}Fe$	$^{54}Fe(^3He,d)^{55}Co$	$^{54}Fe(^3He,\alpha)^{53}Fe$	$^{54}Fe(\alpha,p)^{57}Co$
$\frac{1}{3}$ height determination	1	0.5	0.8	0.4	0.7	1.0	0.7	1.2	0.9
$\Delta\rho = 0.022$ mm	1	0.4	0.5	0.4	0.5	0.5	0.4	0.6	0.4
Peak width correction	2	0.9	1.1	0.2	1.2	0.7	0.7	1.4	1.0
0.1 mm beam spot shift [b]	2	0.1	0.2						
0.02% input energy shift [b]	2	0.7	0.3						
5×10^{-4} rad angle shift [b]	2	0.2	0.2						
Heavy elastic position [c]	2	0.8	0.4	0.7	0.5	1.6	2.7	2.0	1.7
Carbon elastic position [c]	2	0.7	0.8	0.0	0.9	0.0	0.4	0.9	0.8
$\Delta\rho = 0.050$ mm	3	0.2	0.3	0.5	0.0	0.3	0.5	0.1	0.1
$\Delta B = 0.25$ G	2	0.6	0.3	0.9	0.2	0.5	0.0	0.6	0.2
$\Delta B = 0.20$ G	3	0.5	0.3	0.7	0.1	0.4	0.0	0.5	0.2
0.20 mm beam spot shift	2	0.9	0.5	1.4	0.2	1.0	0.0	1.1	0.4
0.15 mm beam spot shift	3	0.7	0.4	1.0	0.1	0.8	0.0	0.8	0.3
0.5 keV error in $^{210}Po(\alpha)$ energy	3	0.4	0.2	0.6	0.1	0.4	0.0	0.5	0.2
Total random error		1.9	1.8	1.8	1.8	2.3	2.9	3.3	2.3
Total systematic error		1.0	0.7	1.5	0.3	1.0	0.5	1.1	0.6
Total uncertainty		2.1	1.9	2.3	1.9	2.5	3.0	3.5	2.4

[a] See text for definition of error types.
[b] Used only if reaction product is not taken in the same run as the heavy elastic.
[c] Used to determine input energy and reaction angle.

confusion for the focused image.[3] As the resulting surface is quite complicated a fourth order power series for each of five sections was required to describe $\rho = \rho(D)$. The 25 parameters are determined by 99 data and the rms deviation of the data is 0.022 mm. This value is taken as the random uncertainty in ρ (item 2 of Table I). The region of the focal surface which is not affected by the exit face modifications requires only a single polynomial. The successive polynomials join smoothly.

The original calibration was taken using ^{210}Po(α) only. However, it was later discovered that the NMR frequency was not exactly porportional to the average magnetic field over the particle trajectory. In order to minimize the effects of differential hysteresis when taking data the magnet is always cycled to a high but subsaturation field and then brought down directly to the required field for the run. During calibration, however, the field was recycled once to the first calibration frequency, and subsequent points were taken by reducing the field in small steps. Unfortunately, for a given NMR frequency differing from the initial calibration frequency these two procedures do not result in the same field. This is determined by noting that the position of a group from a constant energy source does not fall at the same D under these two conditions. If a recalibration is made starting at a different field from the original calibration the resulting curve is displaced from the original by a constant $\Delta\rho$. The magnetic field is thus related approximately to the NMR frequency f by

$$B = 2\pi f/\gamma_p' - f^2 g(f_i)/f_i^2, \qquad (2)$$

where f_i is the first frequency set for a "sufficiently" long time (>30 min) after recycling and γ_p' is the gyromagnetic ratio of the proton in H_2O. In the second term the f^2 insures that $\Delta\rho$ is constant in first order. The arbitrary function $g(f_i)$ is linear to the accuracy we can measure and was determined by recycling to various initial frequencies and determining ΔB from the measured $\Delta\rho$. In Fig. 1 we plot the deviation of the actual field from that calculated from the first term of Eq. (2).

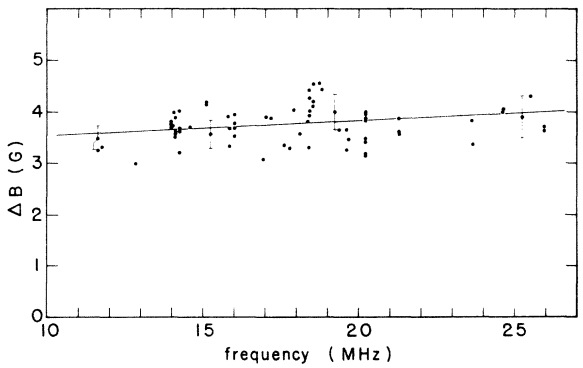

FIG. 1. Data used to find the correction function to the magnetic field, $g(f_i)$ in Eq. (2). The data are taken with $f = f_i$, and the line is the correction applied to the measured field. Representative error bars are indicated.

To determine the ΔB of Fig 1, however, the original calibration curve had to be corrected, as the field had an unknown ΔB when it was measured. This offset can be found by measuring the positions of two well-known groups simultaneously as the ratio of magnetic rigidities, $R = (B\rho)_1/(B\rho)_2 = \rho_1/\rho_2$, is independent of B. Then by displacing the calibration curve, $\rho \to \rho + \Delta\rho$, the experimental ratio can be adjusted to the known value. For these measurements we used ^{210}Po(α) and ^{212}Po(α) in two sets of runs. In the first, two sources were alternated without changing B, and in the second, a single source on which both ^{212}Po and ^{210}Po had been deposited, was used. These measurements leave residual $\Delta\rho = \pm 0.05$ mm and $\Delta B = \pm 0.2G$ uncertainties in the correction and indicate a $0.25G$ uncertainty in resetting a field (items 9, 10, and 11 in Table I).

Figure 2 shows that the measured R is independent of position. Thus the focal surface determined by stepping the field, as explained above, is the same as that using various energy particles at a single field—the normal running condition. A check of the validity of the above procedure was made by simultaneously measuring the positions of doubly and triply charged ^{6}Li groups elastically scattered from Au. The measured ratio is 1.500 07 ±0.000 07, where the uncertainty is the rms deviation of eight measurements. The result is in excellent agreement with the expected value of

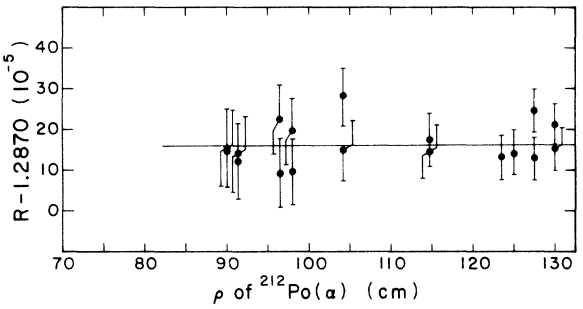

FIG. 2. Measured ratio of ^{212}Po(α) to ^{210}Po(α) rigidities as function of focal surface position. Note the suppressed zero. This data determined the $\Delta\rho$ error in the original calibration curve. For the lowest points the ^{210}Po(α) is at $\rho \simeq 70$ cm, the lower limit of the focal surface. The line is the ratio $R = 1.28716$, from Ref. 4, and the fact that the measured ratio is independent of position indicates that the focal surface is actually defined by the calibration procedure.

1.500 068 affirming the correctness of the calibration curve.

Throughout the calibrations the α-source energies were assumed to be those measured by Rytz.[4] However, we cannot guarantee there is not some energy loss in the sources we used. The narrowest ^{210}Po(α) source peak observed, under special conditions, was 1 keV full width at half-maximum (FWHM). As there are certainly other contributions to this width, we feel that 0.5 keV is a conservative estimate of the energy uncertainty in the sources as used (item 14 in Table I).

If the beam spot shifts vertically the image will also move. We assign a 0.2 mm random uncertainty and possible 0.15 mm systematic shift (items 12 and 13 of Table I.)

B. Peak position determination

The response of the spectrograph to a monoenergetic source 0.5 mm high was determined from the calibration peaks and found to be a skewed triangle with a FWHM $\simeq$ 1.5 mm which is independent of D. As seen in Fig. 3, the experimental peaks are often wider and the different reaction products have different widths indicating that corrections are necessary.

1. Third-height determination

Experience has shown that measurements of the position of a strong peak, at least 75 counts per $\frac{1}{2}$ mm strip at the peak, can be reproduced to about 0.1 mm. We use the algorithm $\Delta D = \min(\text{FWHM}/15; 0.4\text{ mm}) \times \max[(225/N)^{1/2}; 1]$ where N is the number of counts in the peak. The maximum uncertainty is limited because a broad peak has a flat top and only the width of the leading edge is then important. The corresponding uncertainty in energy is the first item in Table I.

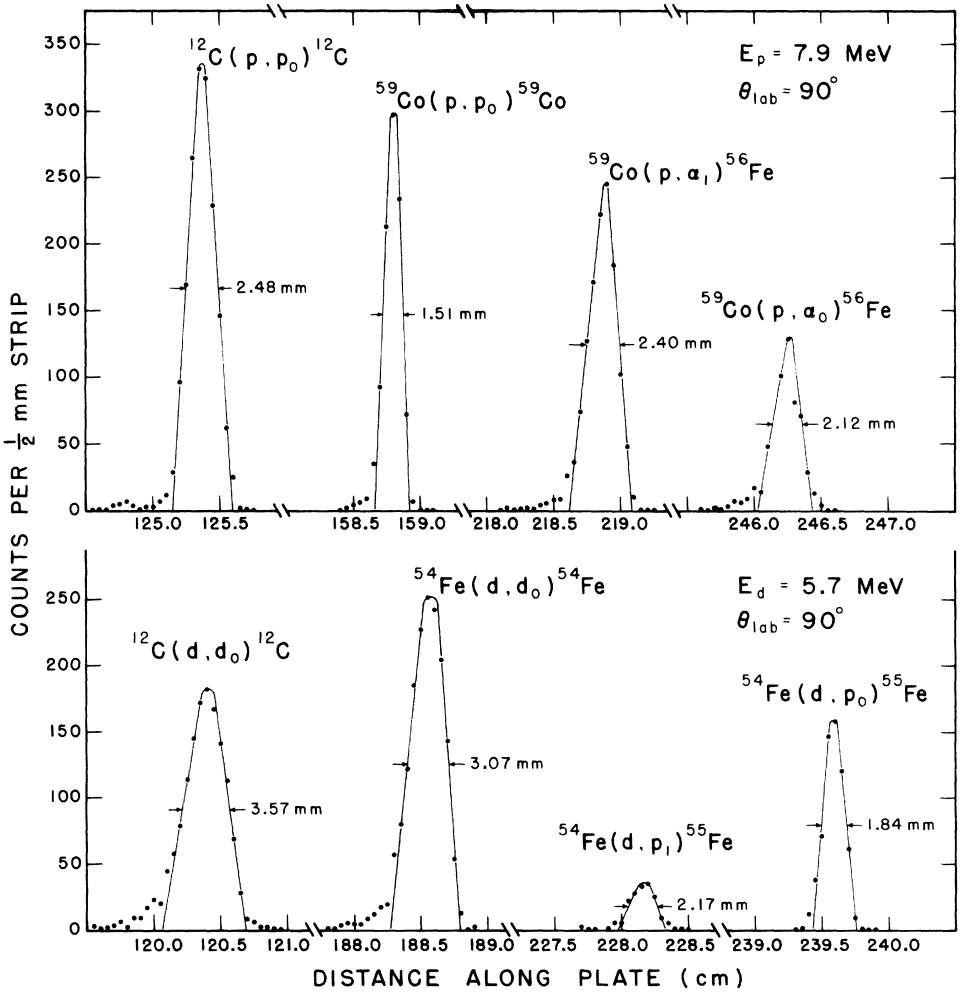

FIG. 3. Two sets of typical data. Note the variation in peak width for which corrections must be made.

2. *Peak broadening*

The physical effects that broaden the peak also alter the position of the third height. The effects considered were the spread in beam energy, the angular convergence of the beam and divergence of the outgoing particles, and the stopping in the target. The beam energy spread is approximately symmetric so the first three effects spread the peak symmetrically about its center whereas stopping also shifts it to lower energy. Of these variables only the outgoing angular divergence which is defined by the spectrograph is measured independent of the peak shape. If the beam energy spread is small the peak shape is well reproduced by a double convolution of the intrinsic triangular peak shape with rectangles for the two angular divergences. In the experiments $dE_{\text{out}}/d\theta$ is relatively large for the group elastically scattered from carbon (the stopping is calculated from the nominal foil thickness) and thus the angular convergence of the beam can be determined. The stopping in the heavy target material can be found as it is the dominant contribution to the width of heavy particle groups, such as α particles. Beam energy spread contributes importantly to groups of the lightest particles, e.g., protons or deuterons. Thus all three parameters could be calculated by simultaneously fitting the FWHM of all the peaks. The resulting position corrections were less than 1 mm and were assigned a 25% uncertainty. This is related to the FWHM and the algorithm used was min[(FWHM-1.5 mm)/3; 0.3 mm] where the upper limit again reflects the importance of only the leading edge width for broad peaks (item 3 of Table I).

3. *Shifts between runs*

If all the groups are not recorded simultaneously, and since the carbon elastics were always recorded in a separate run, there could be small shifts in the beam energy or position. We assigned a ΔE of $\pm 0.02\% E$, i.e., 40% of the analyzing magnet resolution, and $\Delta\theta = \pm 5 \times 10^{-4}$ rad, a typical value for

TABLE II. Q values measured in this work and comparison with the Wapstra-Gove values.

	Reaction	Number of runs	Q (keV)	Random uncertainty (keV)	Systematic uncertainty (keV)	$Q - Q_{WG}$	χ^2	Q-value shift from 5 μg/cm^2 C buildup	References for excited states [a]
1	^{54}Fe$(p,\alpha)^{51}$Mn	4	−3146.9 ± 1.1	0.8	0.7	1.1	0.05	3.1	6
2	^{56}Fe$(p,\alpha)^{53}$Mn	6	−1052.0 ± 0.8	0.8	0.2	6.6	5.14	2.6	7
3	^{59}Co$(p,\alpha)^{56}$Fe	4	3240.4 ± 1.4	1.2	0.7	2.5	0.64	2.3	8
4	^{58}Ni$(p,\alpha)^{55}$Co	4	−1335.1 ± 0.9	0.9	0.3	23.2	33.60	2.2	
5	^{60}Ni$(p,\alpha)^{57}$Co	4	−263.6 ± 0.7	0.7	0.1	4.3	1.83	3.0	9
6	^{62}Ni$(p,\alpha)^{59}$Co	4	343.3 ± 0.7	0.7	0.1	−4.8	4.70	2.8	10, 11
7	^{64}Ni$(p,\alpha)^{61}$Co	4	663.2 ± 0.7	0.7	0.2	−11.8	0.44	2.7	
8	^{12}C$(d,p)^{13}$C	16	2721.9 ± 0.8	0.4	0.6	0.1	0.01	−0.1	
9	^{54}Cr$(d,p)^{55}$Cr	4	4022.1 ± 1.2	0.8	0.8	−13.9	5.16	−0.3	12
10	^{54}Fe$(d,p)^{55}$Fe	5	7072.3 ± 1.7	0.8	1.5	−1.5	0.59	−0.4	13
11	^{56}Fe$(d,p)^{57}$Fe	5	5419.8 ± 1.3	0.7	1.2	−1.7	1.49	−0.4	9
12	^{59}Co$(d,p)^{60}$Co	6	5266.3 ± 1.3	0.7	1.2	−0.6	0.10	−0.3	14
13	^{58}Ni$(d,p)^{59}$Ni	4	6773.5 ± 1.7	0.9	1.4	−1.2	0.37	−0.4	15
14	^{60}Ni$(d,p)^{61}$Ni	12	5596.1 ± 1.3	0.5	1.2	1.2	0.54	−0.3	16
15	^{62}Ni$(d,p)^{63}$Ni	7	4614.0 ± 1.1	0.5	1.0	−2.6	1.65	−0.4	17, 18
16	^{54}Fe$(d,t)^{53}$Fe	2	−7121.5 ± 2.1	1.6	1.4	2.5	0.03	0.4	
17	^{56}Fe$(d,t)^{55}$Fe	6	−4938.3 ± 1.3	0.7	1.0	7.1	6.95	0.4	13
18	^{59}Co$(d,t)^{58}$Co	4	−4196.0 ± 1.4	1.1	0.9	6.7	4.85	0.3	19
19	^{60}Ni$(d,t)^{59}$Ni	4	−5130.2 ± 2.1	1.8	1.1	0.5	0.03	0.3	15
20	^{62}Ni$(d,t)^{61}$Ni	6	−4340.6 ± 1.3	1.0	0.9	−1.6	0.70	0.3	16
21	^{59}Co$(d,\alpha)^{57}$Fe	2	8659.3 ± 3.2	2.6	1.8	−0.2	0.00	1.6	9
22	^{60}Ni$(d,\alpha)^{58}$Co	3	6084.5 ± 2.2	1.7	1.3	5.2	1.35	1.8	19
23	^{62}Ni$(d,\alpha)^{60}$Co	2	5611.2 ± 2.4	2.1	1.3	−3.8	1.67	1.9	14
24	^{54}Fe$(^3$He$,d)^{55}$Co	2	−426.9 ± 2.2	2.1	0.4	16.9	29.51	−2.1	
25	^{54}Fe$(^3$He$,\alpha)^{53}$Fe	2	7199.6 ± 2.6	2.3	1.1	2.6	0.03	0.2	
26	^{54}Fe$(\alpha,p)^{57}$Co	2	−1770.3 ± 1.8	1.7	0.6	−1.4	0.21	2.5	9
27	^{59}Co$(\alpha,p)^{62}$Ni	1	−346.5 ± 2.3	2.3	0.2	1.6	0.26	2.7	20
28	^{12}C$(p,p)^{12}$C	12	−4439.0 ± 1.1	0.5	1.0			0.1	
29	^{12}C$(d,d)^{12}$C	12	−4440.5 ± 1.1	0.7	0.9			0.1	
	^{12}C (average)	24	−4439.5 ± 1.0	0.4	0.9			0.1	

[a] This column gives the sources for the excitation energies of low lying excited states for which Q values were measured in addition to the ground state Q value.

TABLE III. Summation of reaction chains.

Reaction chain [a]	Residual particles	$\sum Q$ (keV)	$\sum Q_{\text{theory}}$ (keV)	σ_{total} (keV)	σ_{random} (keV)	Δ (keV)	Δ_{CBU} [b] (keV)
6+12−23		−1.6	0.0	2.8	2.3	−1.6	−1.3
10−17−3−6+20−14 +19−13+4−24	$d+\alpha-{}^3\text{He}-t$	−14322.0	−14320.9	4.9	3.7	−1.1	−1.3
4−24+26−5+19−13	$d+\alpha-{}^3\text{He}-t$	−14318.6	−14320.9	4.5	3.6	2.3	4.6
10−17−3−6+20−14 +5−26		−3.4	0.0	3.8	2.8	−3.4	−5.8
20−14+22−18+12 −23		−1.1	0.0	4.2	3.2	−1.1	−1.1
3+11−21		0.9	0.0	3.7	3.0	0.9	1.1
5−26+10−17−3+18 −22		−3.9	0.0	4.2	3.2	−3.9	−5.1
20−14+22−18−6		0.5	0.0	3.3	2.4	0.5	0.1

[a] Numbers correspond to reactions in Table II and Fig. 4.

[b] The difference between the calculated and theoretical closures if our Q values had been adjusted for a 2.5 μg/cm^2 carbon buildup on the targets.

the change in angle between two successive Q-value measurements. In addition, we assume a possible 0.1 mm vertical motion of the beam spot and, if a different plate holder rail is involved, a $\Delta\rho$ = 0.01 mm (items 5, 6, and 4 in Table I.)

4. *Target contamination*

Targets were transferred in air and were not prepared immediately before use. No corrections or separate uncertainties, however, have been included for the effects of target oxidation or dead layers on the target surface, as a number of tests indicate that the effects are small. Uniform oxidation throughout the target would cause greater energy loss, but this will be properly accounted for in the target thickness correction described above. Partial oxidation or a carbon or oil buildup on the target would not have quite the same effect. The chamber used was quite clean and no carbon buildup was observed. A buildup of 5 μg/cm^2 of carbon is enough to be observed visually and the effect of partial oxidation might be as large, since the targets were all $\simeq$20 μg/cm^2. In column 9 of Table II the Q-value shift that would be produced by a 5 μg/cm^2 carbon layer is indicated. The correction is significant only for reactions involving helions but would, in general, force our measurements away from the Q values of WG. Also, if a correction of one half the value in the table is applied, the consistency tests described below are not as satisfactory; see Tables III and IV. One reason for the lack of an observable effect is that the target thickness correction also partially compensates for a dead layer. The energy loss is small for 5 μg/cm^2 of carbon, <5 keV, and the straggling is thus

TABLE IV. Comparison of (d,p) and (n,γ) Q values.

Target	$Q(n,\gamma)$ [a] (keV)	Δ [b] (keV)	χ^2	$Q(n,\gamma)$ [c] (keV)	Δ [b] (keV)	χ^2	Ref. [c]
^{12}C	4946.24 ± 0.25	0.3	0.08				
^{54}Cr				6246.3 ± 0.4	0.4	0.10	12
^{54}Fe	9298.7 ± 1.0	−1.8	0.83	9298.1 ± 0.7	−1.2	0.42	21
^{56}Fe	7646.0 ± 0.5	−1.6	1.32				
^{59}Co	7491.5 ± 1.5	−0.6	0.09	7491.1 ± 1 [d]	−0.2	0.01	22
^{58}Ni	8999.4 ± 1.0	−1.3	0.43				
^{60}Ni	7819.5 ± 1.0	1.2	0.53	7819.5 ± 0.8	1.1	0.52	17
^{62}Ni	6840 ± 2	−1.4	0.38	6838.2 ± 0.7	0.4	0.09	17
	$\langle\Delta\rangle$ = −0.74 keV			$\langle\Delta\rangle$ = 0.1 keV			
	Most precise data $\langle\Delta\rangle$ = −0.26 keV						

[a] Data from Ref. 1.

[b] $\Delta = Q(d,p) - Q(n,\gamma) + 2224.6$ keV.

[c] Later more precise data than Ref. 1.

[d] The uncertainty is not given in Ref. 22 but is estimated to be <1 keV.

large, >50%. Consequently the targets will appear thicker than they actually are in our analysis and partial compensation of 30–50% will occur. Finally, several targets were reused after a lapse of more than one month with no significant change in the Q values measured.

IV. Q VALUE RESULTS

Our results are given in Table II and compared with the Q values of WG. About one fourth of our measurements are inconsistent with WG, which is not statistically significant. In some cases, however, the discrepancy is quite large and in two cases (reactions leading to ^{55}Co and ^{55}Cr) it appears that a measurement included by WG was incorrect. Some of the other discrepancies may be due to the ^{57}Fe mass doublet discussed by WG and below. The ^{58}Ni(p, α)^{55}Co Q value of this work entirely supercedes that of Ref. 2. The present number is 6 keV farther from the 1971 value, and the change is due to the target stopping correction which, as noted in Ref. 2, was not considered.

V. CONSISTENCY CHECKS

A number of checks were performed to determine if the data are internally consistent within the errors assigned and externally consistent with previous data. In averaging the Q values over different final states in a single run the average weighted variance ($w = \chi^2$/number of degrees of freedom) was $w = 0.8$. In averaging between runs $w = 0.5$. As there are about 100 degrees of freedom in each case this indicates that the random uncertainties are possibly over estimated.

In two cases we measured parallel reactions. The first is ^{62}Ni(p, α)^{59}Co and ^{59}Co(α, p)^{62}Ni. There is only a single (α, p) run, however, and the statistics are inadequate. The measurements are consistent although the agreement is not as good as we would like. The other case is the (d, t) and (^{3}He, α) reactions on ^{54}Fe, where the agreement is excellent, and, as there are two runs of each reaction, more significant.

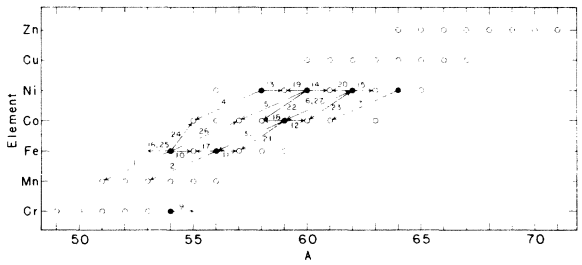

FIG. 4. Map of the region investigated in the present work. Circles ○ indicate primary nuclei. The circles are filled in for the targets used. Arrows indicate Q values measured, and the solid arrows indicate the reactions in the interconnected set used in consistency checks. The numbers correspond to the reaction list in Table II and are useful in interpreting Table III.

Another set of tests was carried out on the closed, connected subset of our data shown in Fig. 4 (see Table III). First the Q values were summed about the loops indicated in the table and the results compared with the expected values. For example, the Q values forming the loop ^{62}Ni(p, α)-^{59}Co + ^{59}Co(d, p)^{60}Co – ^{62}Ni(d, α)^{60}Co, reactions 6 +12 – 23 in the terminology of Tables II and III, should sum to zero. We find the sum from our measurements to be –1.6 keV, and the rms sum of the errors is 2.8 (2.3) keV if the total (random) uncertainties are used. In this procedure the expected values of those loops that do not close to zero are found from the masses of a few light nuclei and they should have little error. The agreement is good within the uncertainties (Table III).

Finally, a mass adjustment was made using the data of Table II, keeping ^{56}Fe fixed to provide a zero and using only the random part of the assigned error. The result gave $\chi^2 = 4.34$ for six degrees of freedom. This is a very stringent test as the systematic errors need not cancel even though only our Q values are used, and the result indicates, as above, that the random uncertainties are overestimated by $\simeq 40\%$. It is difficult to determine whether a few or all of the random errors are too large. The assigned values are our best estimates.

The existence of precise (n, γ) values which parallel our (d, p) measurements provides a close external check for systematic uncertainties. The comparisons are listed in Table IV. If we select the most precise (n, γ) values in the table, then for eight Q values, $\chi^2 = 2.97$. If we use only the random part of our error the $\chi^2 = 7.62$. Further the average of our (d, p) values lies only 0.26 keV below the Q values calculated from the (n, γ) measurements. (If only the WG data is used the value is –0.74 keV.) These facts indicate that our systematic error is perhaps overestimated. Also many of the contributions to the systematic uncertainty are larger for (d, p) Q values than other measurements.

Another paper, in preparation, comparing excitation energies measured by γ decay with values obtained with the 100 cm spectrograph will also indicate very small systematic errors. We include the excitation energy of the first excited state of ^{12}C as an example as the measurements were made simultaneously with the Q values. The agreement between (p, p) and (d, d) is very good. The average agrees with the corrected γ-ray values in Nolen *et al.*[23] as well as with their value from a charged particle measurement. The mass adjust-

ment discussed below provides another check for systematic differences.

VI. MASS ADJUSTMENT

In order to determine the effect of our measurements on the masses of the nuclei involved and further check the data's consistency, we performed a mass adjustment in a limited region centered on Co. We adjusted the masses of all the primary nuclei of the 1971 evaluation for the elements from Cr to Zn inclusive, using all the input data of WG plus our Q values. While we did a least squares fit, as did WG, there are a few differences that should be noted. First, we assumed all masses that were not adjusted to have no error. This will cause some distortion but the buffer around the nuclei we actually measured, created by including a fairly large number of extra nuclei on each end of the region, should minimize such effects. If only the WG data are used to adjust the region no mass differs from WG by more than 0.7 keV, which is some indication of the truncation error. Also, as we wanted to observe the effect of our data, we did no preaveraging of parallel reactions, e.g. (d, p) and (n, γ), between our data and that of WG, although we retained all of their preaverages. The results of the various fits described below are found in Table V.

Before discussing the fits including our data some remarks about the WG data in this region are needed. There are 129 data and 52 variable masses. However, $\chi^2 = 112$ for a weighted variance of $\simeq 1.5$, indicating possible inconsistencies in the data. We can reduce w to 1 by removing only two values, the $^{55}Cr(\beta^-)^{55}Fe$ value and the ^{57}Fe mass doublet discussed in WG. The first of these is relatively unimportant, having almost no effect on masses other than ^{55}Cr. Our $^{54}Cr(d, p)^{55}Cr$ value is in disagreement with both WG values and has a small uncertainty. It does agree with a very precise (n, γ) value recently published.[12] Consequently the β-decay number should be removed from the set. This removes ^{55}Cr from the class of primary nuclei and so it has not been included in the fits below.

The C_7H_8-$^{57}Fe^{35}Cl$ mass doublet measurement has more far reaching effects because there are a large number of precise reaction Q values involving ^{57}Fe. This datum has a $\chi^2 = 16.5$ and this prompted WG to point out that it is inconsistent with other mass doublet measurements in the region. WG included the datum in their fit as they apparently could not determine if this measurement was incorrect or if the other doublets had a systematic error. They did not point out explicitly, however, that if this single datum is excluded the masses of $^{56,57,58}Fe$ and $^{56,57,58}Co$, using our truncated region, all increase by more than 5 keV, or about twice the stated uncertainty, because of the precise reaction measurements between them. This effect lessens farther from ^{57}Fe but some

TABLE V. χ^2 for mass adjustments with various data sets.

	Data used		χ^2 for selected data						
	Ref. 1	Present work	$^{55}Cr(\beta^-)^{55}Mn$	$^{55}Co(\beta^+)^{55}Fe$	^{57}Fe doublet	$^{55}Mn(p,\gamma)^{56}Fe$	χ^2	Degrees of freedom	No. of variables
1	×		14.2	0.0	16.5	3.6	111.9	77	52
2	×		a	0.0	16.0	4.0	96.6	76	51
3	×		a	b	16.1	4.0	96.6	75	51
4	×		a	b	b	6.5	75.8	74	51
5	×		a	b	b	b	66.2	73	51
6		× [c]					3.4	6	13
7		× [c]					3.3 [d]	6	13
8		× [e]					4.3	6	13
9		× [e]					5.1 [d]	6	13
10	×	×	18.8	26.3	21.5	10.8	194.0	101	52
11	×	×	a	25.9	21.4	11.1	172.9	99	51
12	×	×	a	b	21.1	8.7	131.6	98	51
13	×	×	a	b	b	9.1	107.4	97	51
14	×	×	a	b	b	b	97.5	96	51
15	×	×	a	b	b	b	103.1	96	51

[a] Fit does not include ^{55}Cr as a variable and all data leading to ^{55}Cr are removed.

[b] Datum deleted.

[c] Fit uses only the data in the interconnected loop; see Fig. 4. The mass of ^{56}Fe is held fixed.

[d] Same conditions as preceding fit except the Q values of the present work have been adjusted for a 2.5 $\mu g/cm^2$ carbon layer on the surface.

[e] The same as c, but only the random part of the uncertainty is used.

change persists throughout the region.

When our 26 data are added to the WG set there is an increase to $w \simeq 1.9$. By removing the ^{55}Co-$(\beta^+)^{55}$Fe datum of WG we again have $w \simeq 1.4$. As our two data leading to ^{55}Co and a recent ^{54}Fe-$(p,\gamma)^{55}$Co measurement by Martin *et al.*[24] agree, we conclude that the β^+ measurement is in error, although the reason is not obvious.

Our measurements do not bear directly on the believability of the ^{57}Fe mass doublet. What we can hope to do is reduce the uncertainties in Q values so that the quality of the comparison between the doublet in question and many other doublets is improved. That is, while a comparison between the doublet measurements in ^{56,57}Fe may not conclusively indicate which is wrong, if all doublet measurements for $50 < A < 60$ could be compared the question might be resolved. When our data are added, the χ^2 for the ^{57}Fe doublet increases from 16 to 21. Thus the closer ties to many other mass doublets due to our measurements indicate that the ^{57}Fe value is inconsistent with a large set of other doublets. However, at the same time the ^{55}Mn and ^{59}Co doublets do not fit as well when our data are used, although the χ^2 contribution of all doublets is not significantly changed. For the WG data set the weighted variance drops from 1.3 to 1.0 when the doublet is removed. When our data are added the drop is from 1.3 to 1.1, although the reduction in χ^2 is slightly larger. The effects of the truncated space are more important when our data are added, as the more precise Q values allow less relative movement in the center section.

Another approach is to examine reactions between one of the nuclei ^{56,57,58}Fe, ^{56,57,58}Co, which are tied together as described above, and a nucleus outside the set. In Table II we see that a number of such reactions, e.g., ^{56}Fe(p,α) and (d,t), disagree with the WG Q values. However, in fit number 14 where the ^{57}Fe doublet is excluded,

TABLE VI. Mass excesses for nuclei varied in the fits of Table V.

A	Element	Mass excess (keV)	Uncertainty [a] (keV)	$M-M_{71}$	Uncertainty in M_{71} (keV)
49	Cr	−45 388	10	0	10
50	Cr	−50 255.8	1.3	−0.1	1.9
51	Cr	−51 446.0	1.0	0.0	1.8
	Mn	−48 239.4	2.2	0.6	5
52	Cr	−55 414.9	1.9	0.1	2.2
	Mn	−50 705.0	3.9	0.0	4
53	Cr	−55 283.7	1.9	0.1	2.2
	Mn	−54 686.7	1.9	−0.2	2.4
54	Cr	−56 932.1	1.9	0.2	2.3
	Mn	−55 555.7	3.9	1.3	4
	Fe	−56 250.6	2.0	1.1	2.7
55	Mn	−57 709.5	2.0	0.5	2.6
	Fe	−57 477.7	2.0	0.7	2.7
	Co	−54 027.5	2.2	−15.1	3.3
56	Mn	−56 908.2	2.1	0.6	2.6
	Fe	−60 603.2	1.8	6.2	2.5
	Co	−56 035.0	2.6	6.2	3.0
	Ni	−53 905	11	3.4	11
57	Fe	−60.177.5	1.9	6.3	2.5
	Co	−59 341.6	1.9	5.4	2.6
58	Fe	−62 149.0	2.1	6.1	2.6
	Co	−59 843.6	2.1	3.6	3.5
	Ni	−60 226.8	2.1	8.2	3.1
59	Fe	−60 661.4	3.3	8.6	3.7
	Co	−62 226.5	1.9	9.2	2.9
	Ni	−61 153.9	2.1	8.7	3.0
60	Co	−61 646.5	1.9	9.1	3.0
	Ni	−64 470.1	1.9	9.1	3.0
	Cu	−58 342.9	4.9	9.1	5
61	Co	−62 901.8	2.9	18.2	18
	Ni	−64 219.4	2.0	7.7	3.1
	Cu	−61 974.2	3.0	7.6	3.8
62	Ni	−66 746.6	1.9	5.3	3.2
	Cu	−62 799.6	4.8	5.4	5
63	Co	−61 856	19	7.0	19
	Ni	−65 514.5	2.1	7.0	3.3
	Cu	−65 580.5	2.1	6.9	3.3
64	Ni	−67 102.9	2.8	6.4	3.8
	Cu	−65 425.1	2.2	6.7	3.4
	Zn	−66 000.6	2.5	5.8	3.4
65	Ni	−65 127.0	4.4	6.0	5
	Cu	−67 259.4	2.9	5.4	3.6
	Zn	−65 908.5	2.8	5.6	3.5
66	Cu	−66 254.4	3.0	5.4	3.7
	Zn	−68 894.2	1.8	0.3	3.6
67	Cu	−67 301.7	7.8	0.3	8
	Zn	−67 876.4	1.6	0.3	3.6
68	Zn	−70 004.1	1.7	0.2	3.5
69	Zn	−68 415.9	2.2	0.3	3.7
70	Zn	−69 559.6	1.5	0.1	3.2
71	Zn	−67 332.1	15	0.0	15

[a] This column does not represent the total uncertainty in the mass as the fitting procedures introduce a systematic bias in the uncertainties, and to a lesser extent in the masses.

and the Fe-Co block then shifts, our measurements have satisfactory variances. The results are not entirely conclusive, but they tend to indicate that the doublet should be discarded. We warn, as WG did, that there may still be systematic errors in the total masses. The relative Q values have been improved, however.

A final questionable datum in WG is the ^{55}Mn-$(p,\gamma)^{56}$Fe value. As seen in Table V, it has a slightly high χ^2 in the 1971 evaluation and any alteration in the data set increases its χ^2. Removal has no large effect on the masses, but we prefer fit number 14 and Table VI gives the masses and changes from WG for this fit. Because we assumed in making the fits that all masses not adjusted, e.g., the V and Ga masses used for some data involving Cr and Zn, respectively, had no error, the resulting masses in Table IV must be used carefully. In particular the uncertainties for extreme A's are unrealistically small.

The masses are systematically higher than the 1971 Mass Table for $56 \leq A \leq 65$. At $A = 56$ this reflects the removal of the ^{57}Fe doublet. Near $A = 65$ there is a decoupling effect because there are no data with small uncertainties that connect nuclei with $A > 65$ to those with $A \leq 65$. This decoupling means our truncation should not seriously bias the data at the upper end. However, only a full fit as performed by Wapstra and Gove and more data near $A = 65$ will show whether the systematic deviation we find is correct. The table is useful in calculating Q values, but not their uncertainties, in the region fitted.

In fits number 14 or 15 our data has an average variance of slightly less than the rest of the data, indicating good agreement, and we conclude that the errors in the present work are properly described by our analysis.

VII. SUMMARY

Most of the 27 Q-value measurements reported have uncertainties smaller, and for (p, α) much smaller, than those calculated in The 1971 Atomic Mass Evaluation. Tests indicate that they are self-consistent and, in general, agree with the 1971 values. The (d,p) Q values which range in magnitude from 2.7 to 7.0 MeV, are in excellent agreement with (n,γ) measurements. Our results indicate that the 1971 masses for ^{55}Cr and ^{55}Co are incorrect. The uncertainties for ^{53}Fe and ^{61}Co have been reduced by about a factor of 5. The problem of the ^{57}Fe mass doublet discussed by Wapstra and Gove is not resolved, although indications favor removal of the questionable datum. The absolute values of the masses in the region may still be in error by more than their assigned uncertainties, although the Q values have been improved.

†Work supported by the National Science Foundation under Grant No. GP-27456.

[1]A. H. Wapstra and N. B. Gove, Nucl. Data A9, 265 (1971); A11, 128 (1972).
[2]H. B. Jensen, H. B. Mak, and C. A. Barnes, Nucl. Phys. A185, 209 (1972); A. V. Nero, Nucl. Phys. A185, 213 (1972); R. E. Shamu, E. M. Bernstein, D. Blondin, and J. J. Ramirez, Nucl. Phys. A189, 220 (1972); A. Moalem and B. H. Wildenthal, Phys. Rev. C 8, 1961 (1973); J. D. Goss, C. P. Browne, and A. A. Rollefson, Phys. Rev. Lett. 30, 1255 (1973).
[3]J. D. Goss, A. A. Rollefson, and C. P. Browne, Nucl. Instrum. Methods 109, 13 (1973).
[4]A. Rytz, B. Grennberg, and D. J. Gorman, in *Atomic Masses and Fundamental Constants 4*, edited by J. H. Sanders and A. H. Wapstra (Plenum, London and New York, 1972), p. 1; D. J. Gorman and A. Rytz, C. R. Acad. Sci. B (Paris) 277, 29 (1973).
[5]B. N. Taylor, W. H. Parker, and D. N. Langenberg, Rev. Mod. Phys. 41, 375 (1969).
[6]I. Forsblom, T. Weckström, T. Sundius, G. Bergström, S. Forss, and G. Wansén, Phys. Scr. 6, 309 (1972).
[7]M. T. McEllistrem, K. W. Jones, and D. M. Sheppard, Phys. Rev. C 1, 1409 (1970).
[8]M. N. Rao, Nucl. Data B3 (Nos. 3, 4), 43 (1970).
[9]J. Rapaport, Nucl. Data B3 (Nos. 3, 4), 103 (1970).
[10]J. Vervier, Nucl. Data B2 (No. 5), 1 (1968).
[11]C. P. Swann, Nucl. Phys. A172, 569 (1971).
[12]D. H. White and R. E. Howe, Nucl. Phys. A187, 12 (1972).
[13]R. L. Auble and J. Rapaport, Nucl. Data B3 (Nos. 3, 4), 1 (1970).
[14]A. I. Smirnov, V. A. Shaburov, V. L. Alekseev, D. M. Kaminker, and A. S. Ryl'nikov, Izv. Akad. Nauk. SSSR 33, 1270 (1969) [transl.: Bull. Acad. Sci. USSR 33, 1175 (1969)].
[15]D. M. Van Patter, F. Rauch, B. Seim, Nucl. Phys. A204, 172 (1973).
[16]J. Vervier, Nucl. Data B2 (No. 5), 81 (1968).
[17]J. Kopecky, K. Abrahams, and F. Stecher-Rasmussen. Nucl. Phys. A188, 535 (1972).
[18]J. Bleck, R. Michaelsen, W. Ribbe, and W. Zeitz, Phys. Lett. 32B, 41 (1970).
[19]R. G. H. Robertson and R. G. Summers-Gill, Can. J. Phys. 49, 1186 (1971).
[20]H. W. Jongsma, J. C. de Lange, J. C. Boddendijk, R. Kamermans, and H. Verheul, Nucl. Phys. A150, 520 (1970).
[21]A. M. J. Spits, A. M. F. Op Den Kamp, and H. Gruppelaar, Nucl. Phys. A145, 449 (1970).
[22]E. R. Reddingius, J. J. Bosman, and H. Postma, Nucl. Phys. A206, 145 (1973).
[23]J. A. Nolen, Jr., G. Hamilton, E. Kashy, and I. D. Proctor, Nucl. Instrum. Methods 115, 189 (1974).
[24]D. J. Martin, J. R. Leslie, W. McLatchie, C. F. Monahan, and L. E. Carlson, Nucl. Phys. A187, 337 (1972).